Marine Pollution Bulletin 164 (2021) 111989

Contents lists available at ScienceDirect

Marine Pollution Bulletin

journal homepage: www.elsevier.com/locate/marpolbul

Role of small-sized phytoplankton in triggering an ecosystem disruptive algal bloom in a Mediterranean hypersaline coastal lagoon

Jesús M. Mercado [a,*], Dolores Cortés [a], Francisco Gómez-Jakobsen [a], Candela García-Gómez [a], Sophia Ouaissa [b], Lidia Yebra [a], Isabel Ferrera [a], Nerea Valcárcel-Pérez [a], María López [a], Rocío García-Muñoz [c], Aranzazu Ramos [c], Jaime Bernardeau [c], María Dolores Belando [c], Eugenio Fraile-Nuez [d], Juan M. Ruíz [c]

[a] Centro Ocenográfico de Málaga, Instituto Español de Oceanografía, Puerto Pesquero s/n, 29640 Fuengirola, Málaga, Spain
[b] Programa de Doctorado Diversidad Biológica y Medioambiente, Facultad de Ciencias, Universidad de Málaga, Campus de Teatinos, 29071 Málaga, Spain
[c] Centro Oceanográfico de Murcia, Instituto Español de Oceanografía, Varadero 1, Apdo. 22, 30740 San Pedro del Pinatar, Murcia, Spain
[d] Centro Oceanográfico de Canarias, Instituto Español de Oceanografía, C/ Farola del Mar, 22, 38180 Santa Cruz de Tenerife, Spain

ARTICLE INFO

Keywords:
Algal bloom
Diatoms
Dinoflagellates
Eutrophication
Nutrients
Synechococcus

ABSTRACT

Monthly samplings carried out in 2016–2019 and satellite color images from 2002 to 2019 have been combined to determine the onset and causative species of the ecosystem disruptive algal bloom (EDAB) that affects the Mar Menor coastal lagoon (Western Mediterranean Sea) since 2015. Substantial changes in satellite spectral reflectance attributable to increasing abundance of *Synechococcus* were registered in 2014. Furthermore, cell abundances of this species in 2016 were the largest ever obtained in the lagoon (6 10^6 cells mL^{-1}), with values similar to those reported for other Mediterranean hypertrophic estuaries and coastal lagoons. These results suggest that the early changes leading to the EDAB started in 2014 and that *Synechococcus* played a relevant role in its development. Moreover, diatom and dinoflagellate abundances changed substantially in 2016–2019, ranging from 10^2 to more than 10^4 cells mL^{-1}. Some of these changes were linked to flood, suggesting that EDAB has modified substantially the homeostatic capacity of the lagoon.

1. Introduction

Coastal lagoons are among the most threatened marine ecosystems since human pressures in the catchment areas often release nutrients that may lead to eutrophication (Cloern, 2001), whose effects are amplified by global climate change (Lloret et al., 2008). Numerous studies link eutrophication events in coastal areas with the increasing incidence of long-term harmful algal blooms that disrupt or degrade the structure and function of the ecosystem (the so called 'ecosystem disruptive algal blooms', EDABs; Lomas et al., 2004; Sunda et al., 2006). In coastal lagoons, where macrophyte communities play a key role in maintaining the ecological balance (McGlathery et al., 2007), EDABs produce benthic-pelagic mismatches that contribute to the collapse of the ecosystem (Glibert et al., 2010; Fertig et al., 2013). The species known to cause EDABs belong to fairly dissimilar taxa, including cyanobacteria (*Synechococcus* and *Nodularia spumigena*), pelagophytes (*Aureoumbra lagunensis* and *Aureococcus anophagefferens*), trebouxiophyte (*Nannochloris atomus*), eustigmatophyte (*Nannochloropsis*), haptophytes (*Chrysochromulina polylepis* and *Prymnesium parvum*) and dinoflagellates (Liu and Buskey, 2000; Trice et al., 2004; Sunda et al., 2006; Michaloudi et al., 2008; Sunda and Shertzer, 2012; Majaneva et al., 2012; Zhang et al., 2015). According to Sunda et al. (2006), all these species producing EDABs share as a common feature their small size and, possibly, their ability for using organic nutrient forms, given that their capacity for assimilating inorganic nutrients is not higher than in other species causing blooms. Some reports also suggest that their toxicity or low palatability for herbivore predators may contribute to the disruption of the trophic dynamics (Sunda and Shertzer, 2012). Consequently, not only the available nutrients but also the trophic interactions may be key factors in determining the triggering of the EDABs. In turn, the diversity of species causing EDABs could imply that the specific environmental factors triggering the bloom differ from one to another coastal system. The EDABs species identification is therefore essential to understand the origin of a disruptive event and,

* Corresponding author.
E-mail address: jesus.mercado@ieo.es (J.M. Mercado).

https://doi.org/10.1016/j.marpolbul.2021.111989
Received 3 August 2020; Received in revised form 23 December 2020; Accepted 24 December 2020
Available online 20 January 2021

ultimately, to implement effective management strategies (Cloern, 2001).

One of the most recent EDABs reported in the Mediterranean Sea has occurred in the Mar Menor, the largest hypersaline lagoon in the Western Mediterranean Sea, where strong deterioration of the water quality and benthic communities was appreciated for the first time in 2016 (Belando et al., 2019a; Erena et al., 2019; Pérez-Ruzafa et al., 2019). Previously, the Mar Menor lagoon was classified as an oligotrophic system with chlorophyll concentrations in the water column being normally below 1 μg L^{-1} (Más-Hernández, 1996; Gilabert, 2001; Pérez-Ruzafa et al., 2005; Lloret et al., 2008). Extensive presence of benthic macrophyte communities that in fact covered almost 100% of the bottom was another singular feature of the lagoon (Terrados and Ros, 1991; Belando et al., 2019b). The reduction of the water quality detected at the end of 2015 was accompanied by a drastic decrease in water transparency and an increase in chlorophyll concentration above 15 μg L^{-1} in 2016 (Fraile-Nuez et al., 2018; Belando et al., 2019a; Erena et al., 2019; García-Oliva et al., 2019; López-Ballesteros et al., 2019). Since then, a strong deterioration of the macrophyte communities has occurred, leading to a reduction of 85.8% in 2016 (Belando et al., 2019b). Although the first symptoms of this episode were detected in 2015, samplings aimed at describing the causes did not start until the second quarter of 2016, when the deterioration of the water quality was already critical. Consequently, the exact onset of the EDAB as well as the causative species during the initial phase have not been determined. Some published data on the phytoplankton composition from May to December of 2017 indicate that the abundances of *Synechococcus*, Chlorophyceae, Chrysophycea and nanoplanktonic Cryptophycea were higher during that period compared with previously collected data (Soria et al., 2019). These results, together with certain observations in samples collected in 2016 (Ruiz et al., 2016) show abnormal high abundance of small cells which led to the yet unproven hypothesis that the phytoplankton community was dominated by picoplanktonic organisms during the first stages of the bloom.

The main objective of this work is to analyze the dynamics of the phytoplankton community during the early development phases of the ecosystem disruptive event in the Mar Menor lagoon in order to: (1) estimate the onset of the bloom, (2) identify the possible causative species and (3) characterize the subsequent shifts in the community. To complete these goals, satellite color images from 2002 to 2019 were gathered and analyzed in combination with environmental and phytoplankton composition data collected in the Mar Menor lagoon from May 2016 to October 2019.

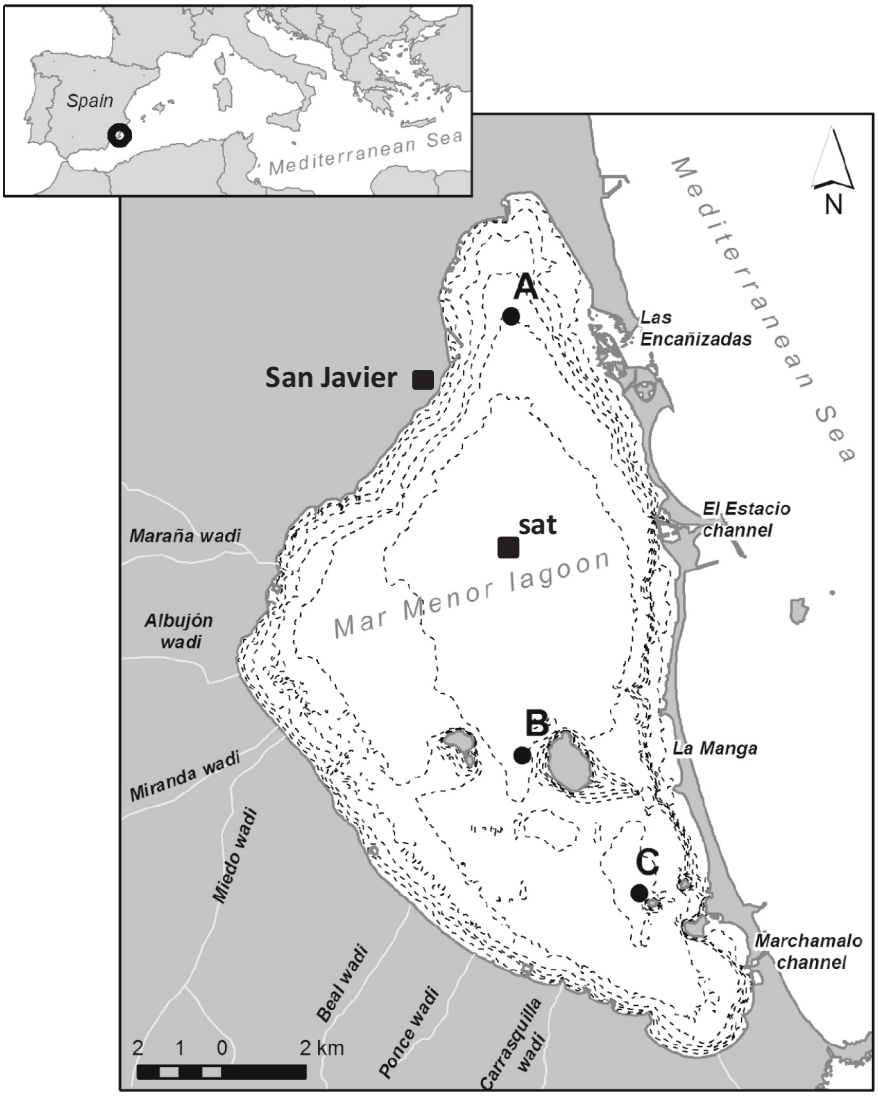

Fig. 1. Map of the Mar Menor showing the location of the sampling stations (A, B and C), the position of the pixel used to build time series of satellite data (sat) and the location of the meteorological station (San Javier).

2. Materials and methods

2.1. Satellite and meteorological data

Ocean color images obtained from the platform MODIS-Aqua were used to retrieve spectral reflectance. The satellite provides a daily image of the study area with a spatial resolution of 1.1 km × 1.1 km. All the Level 2 scenes covering the central part of the lagoon from August 2002 to October 2019 were downloaded from the NASA website (https://oceancolor.gsfc.nasa.gov/reprocessing/r2018/aqua/). Those scenes inadequate for the analysis due to sun glitter and/or the presence of clouds or fog were discarded, and only valid scenes were used. Overall, 1235 daily scenes were used for the analyses. The MODIS sensor provides reflectance values at 412, 443, 469, 488, 531, 547, 555, 645, 667 and 678 nm. The reflectance for each scene was normalized by blue reflectance at 412 or 443 nm (R_n). For our analyses, the reflectance values from the nearest pixel to the center lagoon (Fig. 1; Longitude: −0.789°W and Latitude: 37.735°N) was used to build time series of R_n. This point was located in the lagoon area with maximal depth; therefore, our reflectance time series was not influenced by bottom reflectance as in fact it was assessed by Erena et al. (2019) in their analysis of the satellite images of the Mar Menor in 2017.

Daily data of air temperature near the surface and rainfall from 2002 to 2019 were gathered from the meteorological station of the Spanish Meteorological Agency located just in the shore of the lagoon at San Javier town (http://www.aemet.es; Fig. 1). Atmospheric temperature anomalies were calculated by subtracting the temperature seasonal cycle from the raw time series.

2.2. Samplings and analyses of nutrients, chlorophyll and phytoplankton absorption

Monthly samplings of nutrients and phytoplankton communities were performed in three distinct stations of the lagoon (Fig. 1) from May 2016 to October 2019 (note that samplings could not be performed during some monthly periods due to weather conditions). At each point, samples were collected by triplicate with Niskin bottles at 3–4 m depth. Previous samplings indicated the absence of any kind of water column stratification so that samples collected at that intermediate depth can be considered representative of the whole water column. Data of salinity and temperature were taken with a Multiparametric portable meter probe MultiLine® Multi 3620 (WTW-Xylem Analytics, Germany). PAR irradiance profiles were measured each meter from the sub-surface to the bottom with a LI-1500 data logger (LI-COR, Germany).

In the laboratory, water aliquots were either preserved or immediately analyzed depending on the target variable. For nutrient analyses, two replicates of water were immediately frozen at −20 °C. Afterwards, nutrients (nitrate plus nitrite, nitrite, phosphate and silicate) were analyzed by means of segmented flow analysis using a Bran-Luebbe AA3 autoanalyzer, following the methods described in Ramírez et al. (2005). The detection limits were: 0.05 μM for nitrate, 0.01 μM for nitrite, 0.04 μM for phosphate and 0.10 μM for silicate. A total of 0.5 L of water were filtered through Whatman GF/F filters for determination of chlorophyll *a* concentration (Chl *a*) by spectrophotometry after overnight extraction in 90% acetone at 4–5 °C (SCOR-UNESCO 1966). Two-three mL samples were fixed with glutaraldehyde (1% f.c.) and immediately frozen at −80 °C for the counting of picoplankton by means of flow cytometry (Vaulot et al., 1989). Additionally, 250 mL of water sample were fixed in dark glass bottles with Lugol's solution (2% f.c.) for microscopy taxonomic identification analyses.

In addition to the monthly samplings, four intensive surveys were performed in November 2016 and in February, June and September 2017. During these samplings, samples of chlorophyll were collected at 42 stations covering the whole surface of the lagoon at two or three depths depending on the station. These samples were used to obtain light absorption spectra of non-living matter and phytoplankton.

Data of chlorophyll obtained in 2002–2005 from the project EUROGEL (Fuentes et al., 2011) have been also gathered and used for making comparisons with the results obtained from the monthly samplings described above. In the framework of the project EUROGEL, the Spanish Institute of Oceanography performed monthly samplings at 36 stations distributed by the whole Mar Menor. Methods of sampling and analysis of chlorophyll used in that project were similar to the ones previously described.

2.3. Analysis of phytoplankton composition and optical properties

Autotrophic picoplankton was analyzed on a Becton Dickinson FACScan flow cytometer. Counting of cells was performed based on the forward-light scatter (FLS) and the orange and red fluorescence signals. This analysis allowed the identification of *Synechococcus* and eukaryotic picoplankton as the main components of the community. Additionally, Mamiellophyceae were discriminated from other eukaryotic picoplankton according to the FLS signal. Absolute counts were calculated by estimating the flow rates using TruCount™ bead suspensions prepared by adding deionised water to TruCount™ tubes (Becton Dickinson, Franklin Lakes, USA). Abundance of diatoms and dinoflagellates were determined following the technique developed by Utermöhl (Utermöhl, 1958) by settling 50 or 25 mL of each fixed sample in a composite chamber for 24 h. Cells were counted at 200× and 600× with a Nikon Eclipse TS100 inverted microscope. The species nomenclature was validated following Tomas (1997) and the currently accepted taxonomic names were checked in the web site *AlgaeBase* (Guiry and Guiry, 2020). Note that samples collected after January 2019 were not analyzed by microscopy.

Non-living matter and phytoplankton light absorption was estimated with the filter concentration technique by using the procedure described in Mercado et al. (2008). Half liter of seawater was filtered through a glass fiber filter Whatman GF/F and immediately frozen at −20 °C until further analysis in the lab. Absorbance spectra of the particulate matter (OD_{NAP+AP}) were obtained by placing the filters in the optical path of the spectrophotometer (Cary UV–VIS) and measuring the absorbance each nm from 400 to 750 nm against reference of a glass filter wetted with filtered seawater. Later, in order to determine the absorption spectra of the non-living matter, the filters were dipped in 90% acetone and sonicated during 5 min to improve pigment extraction. Pigments were extracted overnight at 4 °C. Afterwards, the filters were air exposed until acetone was evaporated and then were wetted in filtered seawater. Absorbance of the filters after extraction (OD_{NAP}) was measured as mentioned above. A glass fiber filter subjected to the same process was used in the reference cell.

Spectral absorbances of the filters before and after extraction were corrected by absorbance at 750 nm, transformed in absorbance of the suspension (OD_{susp}) using the equation proposed by Cleveland and Weidemann (1993) and then used to calculate absorption coefficients of particulate (a_{NAP+AP}) and non-living (a_{NAP}) matter with the formula:

$$a(\lambda) = 2.3\ OD_{susp}(\lambda)/(V/A)$$

where V is the filtered volume (m^3) and A is the filtered area (m^2).

Absorption coefficient of the phytoplankton [$a_{AP}(\lambda)$ (m^{-1})], was calculated by subtracting $a_{NAP}(\lambda)$ to $a_{NAP+AP}(\lambda)$. Chlorophyll *a* specific absorption spectra [$a^*(\lambda)$ (m^2 mg Chl a^{-1})], were calculated by dividing $a_{AP}(\lambda)$ to Chl *a* estimated from the pigment extracts as described above.

2.4. Statistical analyses

The daily data of satellite reflectance were used to generate monthly time series that were analyzed with the functions *st* and *decompose* of R (R Core Team, 2013). As a result, the monthly time series were split out into seasonal, trend and irregular components. A principal component analysis was performed with the trend series of R_n by using the function

rda with the R-package *vegan* (Oksanen et al., 2014). In order to investigate which variables had more importance in determining the variability patterns of the phytoplankton community, a canonical correspondence analysis (CCA) was performed by using the pool of environmental variables (temperature, salinity and nutrient concentrations) as constraining variables and the chlorophyll *a* and abundances of the different phytoplankton groups (diatoms, dinoflagellates, *Synechococcus*, Mamiellophyceae and other picoeukaryotes) as the constrained variables. R_n of some selected spectral bands were also included into the pool of constraining variables to determine possible associations between the communities and the reflectance signal captured by the satellite. Only the monthly sampling periods for which all the variables were analyzed were used for this analysis. CCA was carried out with the function *cca* of the *vegan* R-package.

3. Results

The analysis of the time series of averaged monthly satellite reflectance at wavelengths representative of the main color bands (R_n488, R_n555 and R_n645) from 2002 to 2019 reveals that the reflectance features of the Mar Menor changed substantially since the last quarter of 2013. Note that these changes were not preceded by remarkable temperature atmospheric anomalies. Since that date, the monthly means of R_n 645 started to increase steeply (Fig. 2) reaching a maximal peak in March 2016. Additionally, high values of R_n488 and R_n555 were obtained in 2014. R_n488, R_n555 and R_n645 decreased substantially since March 2016 until reaching minimum values in 2018. These temporal change patterns in R_n were assessed with a principal component analysis (Fig. 3). The scores of each reflectance band for the first principal component, PC1 (which explained 69% of the variance), were positive indicating that this variance component discriminated monthly means according to the intensity of R_n irrespectively of the spectral band (although the scores of PC1 were comparatively higher for R_n547 and R_n555). The reflectance red bands had positive scores for the second component, PC2 (that explained 29% of variance), while reflectance of the blue bands had negative scores. In contrast, the green bands did not contribute to PC2. The scores of PC1 and PC2 for each monthly period (Fig. 3b) show clearly that PC2 discriminated the observations beginning with April 2014 from the rest of the time series. For that period, PC2 positive scores (i.e. higher contribution of the reflectance red bands) were obtained, with maximal contributions in 2015. Note that PC1 scores decreased progressively after that period.

Monthly means of Chl *a* calculated with data of the three stations sampled from May 2016 to October 2019 are shown in Fig. 4 along the daily data of R_n488, R_n555 and R_n645. Chl *a* ranged from less than 1 to 12 μg L^{-1} for the whole sampling period. The available data for 2003–2004 were close to this lower limit (Fig. 4b). Higher Chl *a* roughly matched with pronounced monthly peaks of R_n645 and R_n667 in 2016–2019. In fact, for that time period, there was a significant correlation between R_n555/R_n645 ratio and Chl *a* (both in logarithmic scales; Fig. 4b), indicating that R_n increasing in the red reflectance bands paralleled the increases in Chl *a* observed during the different phases of the

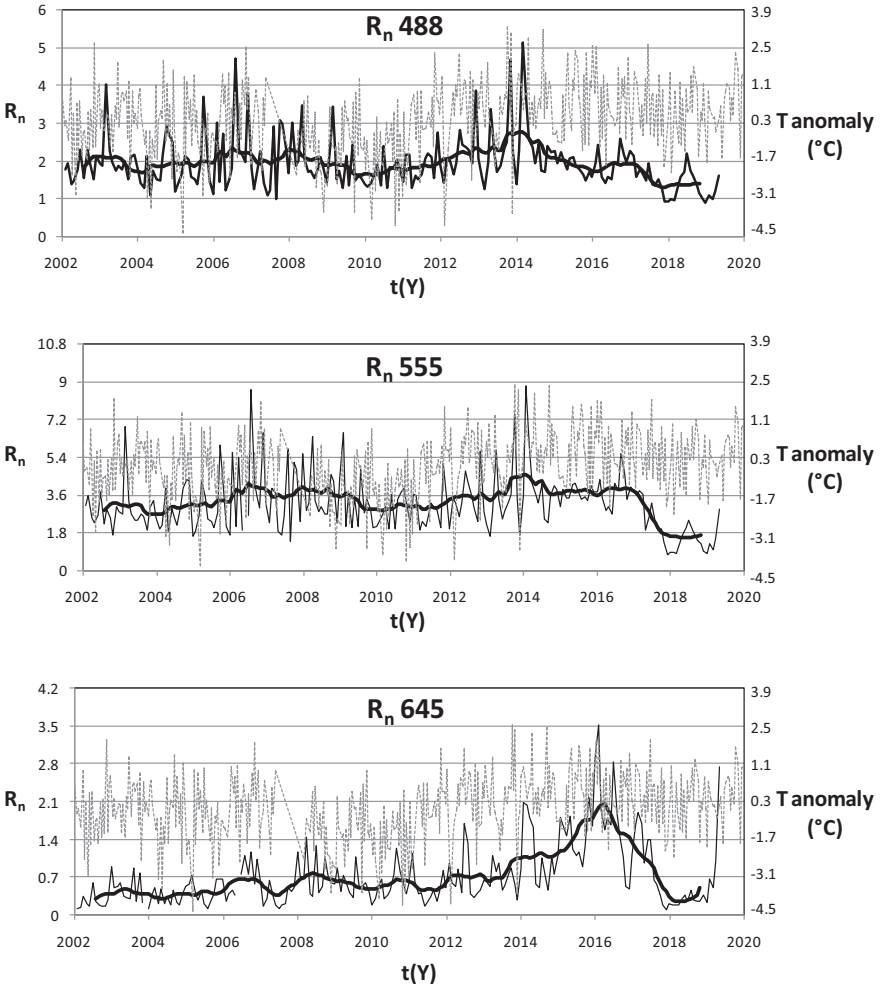

Fig. 2. Monthly mean values of three selected satellite reflectance bands (R_n488, R_n555, R_n645). The thick black line indicates the trend series calculated after seasonal decomposition of the raw series (thin black line). The time series of atmospheric temperature anomalies is also shown (grey dashed line).

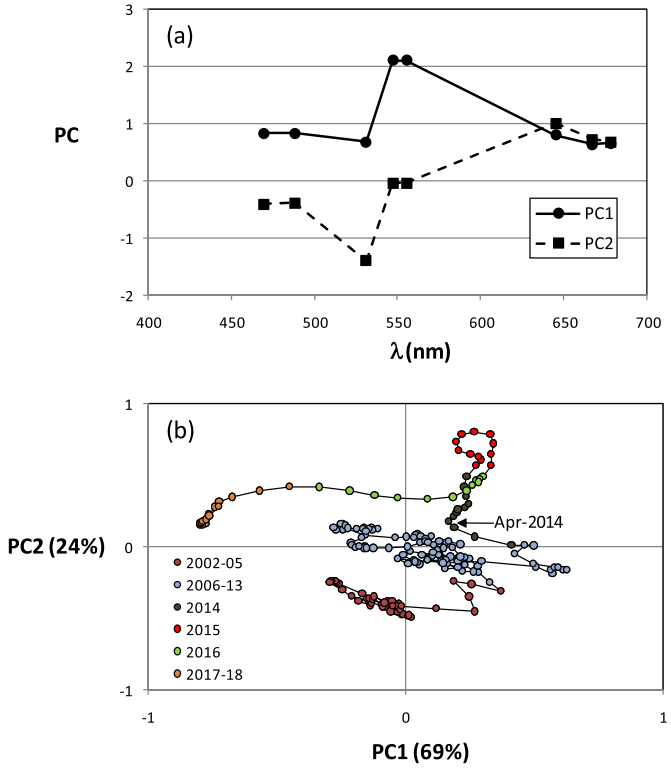

Fig. 3. Results of the Principal Component Analysis performed with the trend series of the different satellite reflectance bands. (a) Two first variance component scores (PC) of each reflectance band; (b) Scores of each monthly period for the two first variance components. Note different colors for each year. (For interpretation of the references to color in this figure legend, the reader is referred to the web version of this article.)

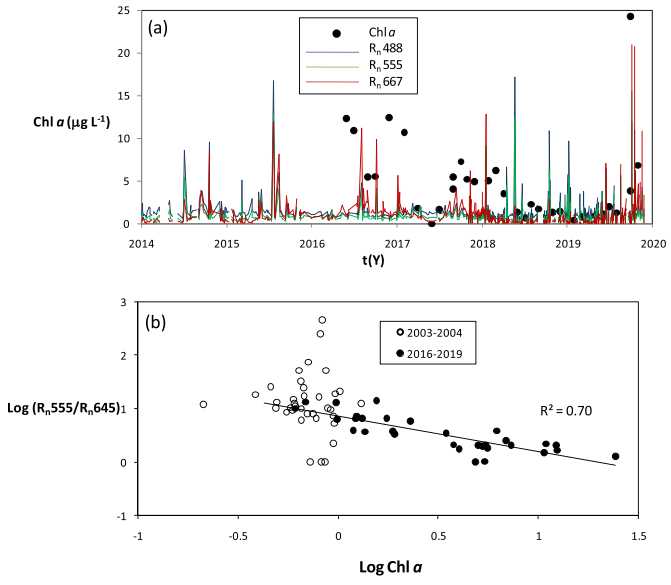

Fig. 4. Time changes in the chlorophyll *a* concentration averaged from the three stations sampled monthly and their relation with satellite reflectance. (a) Monthly chlorophyll *a* (Chl *a*) concentration. Time series of daily R_n at some selected bands obtained during the period 2014–2019 are shown; (b) correlation between chlorophyll *a* (Chl *a*) and R_n550/R_n645 ratio for the period 2016–2019, calculated with the R_n values roughly matching with the sampling date (±48 h).

EDAB. This correlation was not significant in 2003–2004; therefore, the dependence of R_n555/R_n645 ratio on Chl *a* appears to occur exclusively during the EDAB.

As shown in Table 1, the analyzed environmental factors also presented large variation ranges in 2016–2019. Water temperature ranged more than 20 °C, with a minimum in January 2017 coinciding with a flood episode that produced a substantial runoff water discharge from the catchment towards the lagoon and a consequent drastic reduction in salinity. Associated to this heavy rainfall event, high nitrate and low silicate concentrations were obtained at the beginning of 2017. In contrast, the highest phosphate concentrations were obtained in 2018 when silicate also decreased steeply. Note that in that annual period, significant heavily rainfall episodes were absent and salinity remained above 43.0 during all year. Therefore, the changes in nutrient concentrations occurred in 2018 apparently cannot be attributed to significant variations in runoff water discharges.

The abundances of the main phytoplankton groups identified in the monthly samplings are shown in Fig. 5 (note that there are no data for diatoms or dinoflagellates quantified by microscopy after January 2019). Overall, *Nitzschia*, *Cyclotella*, *Cylindrotheca* and *Chaetoceros* were the most abundant genera. The highest abundance of diatoms was obtained at the beginning of 2017 when more than 12,500 cell mL^{-1} were found due to a bloom of *Nitzschia* sp. Since that date, diatom abundance decreased steeply with a minimum in mid-2017. Afterwards, in 2018, some diatom abundance peaks attributable to *Cyclotella* sp. were produced although they were lower than the one occurred in 2017. Dinoflagellates were about one order of magnitude less abundant than diatoms and abundances of the two groups were uncorrelated ($n = 24$; $r^2 = 0.08$; $p > 0.05$). The highest abundance of dinoflagellates was obtained in summer 2016 when the community was dominated by *Prorocentrum*. Dominance of this genus over other dinoflagellates also occurred in different monthly periods of 2017 and 2018. In September 2016 we found that *Gymnodinium* was more abundant than *Prorocentrum* as well as unclassified cells at genus level did in several monthly periods, particularly in 2018.

Abundance of *Synechococcus* ranged by two orders of magnitude (Fig. 6), with maxima up 6 10^6 cell mL^{-1} in August 2016, November 2017 and January 2018. Mamiellophyceae also reached abundance peaks up to 4.5 10^6 cell mL^{-1} in 2016–2017 although this picoeukaryotic group was only present in sufficient abundance for quantification in summer or early fall. The other picoeukaryotes had a variability range comparatively low (from 2.9 10^3 to 7.0 10^4 cell mL^{-1}) and were less abundant than *Synechococcus* in all analyzed samples.

The factors influencing the phytoplankton composition were assessed with a canonical correspondence analysis (CCA, Fig. 7). The two first variance components of the CCA explained 52% and 28% of variability, respectively. Diatoms and Mamiellophyceae had the highest scores for CCA1, although with opposite signs. All samples with positive score for CCA1 presented abundances of diatoms higher than 5.9 10^2 cell mL^{-1} and the samples with the presence of Mamiellophyceae had negative scores. Therefore, CCA1 discriminated the samples mainly according to the relative contribution of both phytoplankton groups. *Synechococcus* presented the highest score for CCA2 followed by Mamiellophyceae also with opposite signs; the scores of the other phytoplankton groups for this variance component were notably low. Therefore, CCA2 discriminated samples according to their *Synechococcus* abundance relative to the other phytoplankton groups. The main environmental variables constraining the phytoplankton community composition were salinity, temperature and nitrate and silicate concentrations; the CCA1 scores for nitrate were positive while for silicate and salinity were negative indicating that, overall, the importance of diatoms was higher when nitrate concentrations increased. In turn, *Synechococcus* was strongly associated with temperature and salinity. It is interesting to note that CCA1 scores of R_n469, R_n531 and R_n555 were fairly low (R_n645 and R_n667 had scores only a little higher) indicating that variability in diatom abundance was barely reflected in the satellite

Table 1
Environmental variables determined during the monthly samplings. The means are average values for the three stations and samples collected at each sampling time. Units: temperature (T), °C; nutrient concentrations, μM; chlorophyll *a* concentration (Chl *a*), μg L^{-1}.

	2016[a]			2017			2018			2019[a]		
	Min	Max	Mean	Min	Max	Mean	Min	Max	Mean	Min	Max	Mean
T (°C)	22.1	27.5	25.2	10.5	30.4	21.9	12.1	29.4	19.9	11.7	29.0	18.5
Salinity	43.6	46.5	45.3	39.3	44.7	42.7	43.3	46.8	44.8	42.9	46.4	44.5
Nitrate	0.35	1.43	0.79	0.06	9.2	3.7	0.15	3.7	1.3	0.04	1.94	0.58
Nitrite	0.02	0.07	0.04	0.07	0.39	0.19	0.02	2.9	0.44	0.13	0.19	0.15
Phosphate	0.02	0.22	0.09	0.04	0.11	0.07	0.03	0.35	0.23	0.11	0.21	0.15
Silicate	23.1	47.0	37.0	12.0	51.1	30.4	0.13	27.2	14.9	0.85	45.3	13.2
Chl *a*	5.0	12.2	9.3	1.5	10.6	3.9	0.6	6.2	2.4	0.4	24.2	4.2

[a] Note that the sampling period was May–December in 2016 and January–October in 2019; therefore, the data do not cover the whole annual cycle.

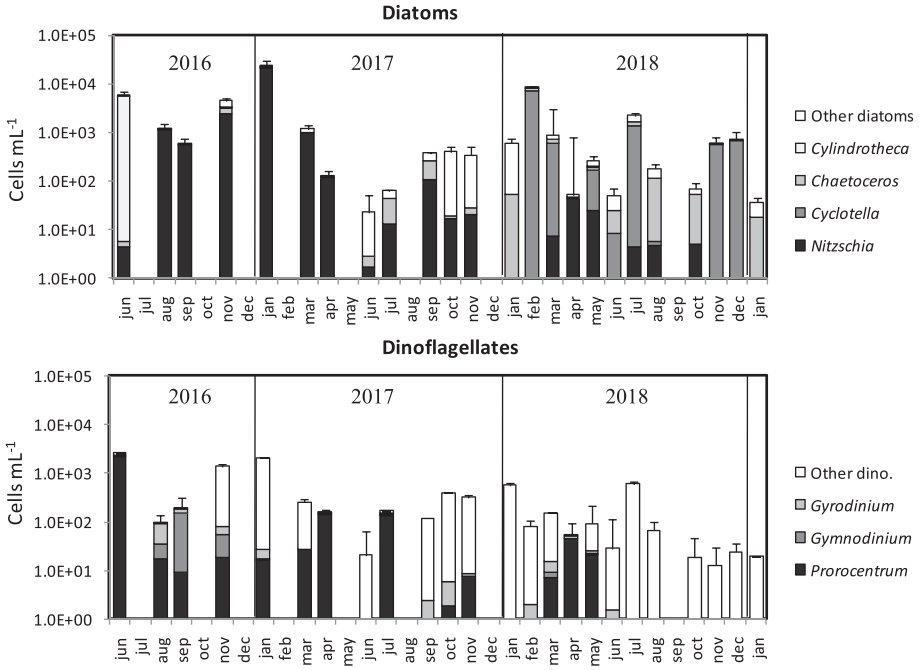

Fig. 5. Monthly mean cell abundances of the main groups of diatoms and dinoflagellates identified in the analyzed samples. Note that the abundances are shown in logarithm scale. Vertical lines on the bars indicate the standard deviation.

reflectance spectra of the Mar Menor. In contrast, all the reflectance bands (apart from R_n555) presented high scores for CCA2 compared to the other variables. Particularly, the CCA biplot indicates that *Synechococcus* was strongly associated to R_n645 and R_n667 suggesting that changes in the relative abundance of this phytoplankton group affected the signal captured by the satellite in these reflectance bands.

In order to assess how the changes in abundance and composition of phytoplankton affected the optical properties of the water column, light absorption spectra of the particulate matter obtained in four intensive samplings performed in 2016–2017 were analyzed (Fig. 8). For the four samplings, the mean spectra showed absorption coefficient peaks in the blue bands at 440, 460 and 495 nm which are attributable to carotenoids absorption. These peaks were more pronounced in November 2016 and October 2017 and less in February 2017 and June 2017 (particularly the absorption peak at 495 nm). Additionally, there were absorption peaks at 545- and 620 nm coinciding with the absorption maxima of cyanobacteria attributable to phycobilins. Note that the absorption percentage by particulate material attributable to non-algal particles (i.e. after pigment extraction) presented minima in the absorption red bands around these peaks (Suppl. Fig. 1), indicating that phytoplankton was the main optical component that contributed to these absorption peaks.

4. Discussion

The anthropogenic pressures on the Mar Menor have increased during the last decades due to population growth and spread of the irrigated agricultural surface area that in fact duplicated from 1988 to 2008 (Carreño, 2015). Leachate from the irrigated area has produced increasing loads of dissolved nitrogen in the ground water that drains into the lagoon; particularly, nitrate has experienced a notable increase with concentrations in ground water of about 22–45 mg L^{-1} (Fraile-Nuez et al., 2018). Heavy rain episodes that feature the Mediterranean weather have also contributed to carry these nutrients from the drainage basin towards the lagoon. Overall, it can be concluded that the lagoon has suffered an eutrophication pressure since the 1980s–1990s that would be aggravated by its low water renewal rate (around 360 days; García-Oliva et al., 2019; Fraile-Nuez et al., 2018). However, as far as we know, visible symptoms of eutrophication such as phytoplankton blooms, reduction in water transparency or decline of the macrophyte communities had not been noticed before 2015 (Erena et al., 2019; Pérez-Ruzafa et al., 2019) and the start date of the lagoon ecosystem deterioration has not yet been determined.

Our data indicate that the satellite spectral reflectance of the Mar Menor changed substantially since 2013 compared to previous periods of the analyzed dataset (2002−2013). Different phytoplankton species

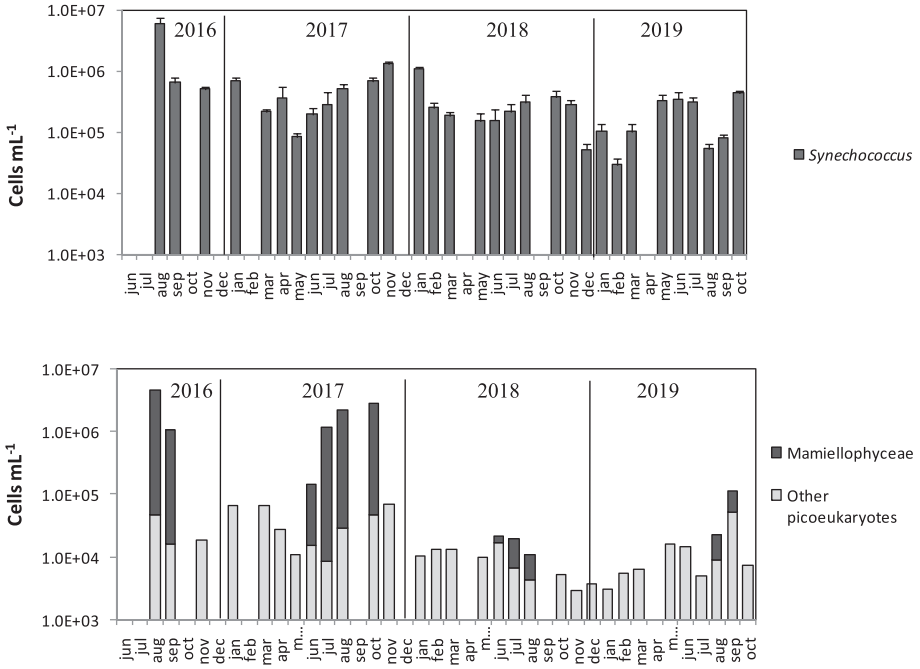

Fig. 6. Monthly mean cell abundances of *Synechococcus* and picoeukaryotes. Note that the abundances are shown in logarithm scale. Vertical lines on the bars indicate the standard deviation of three sampling stations.

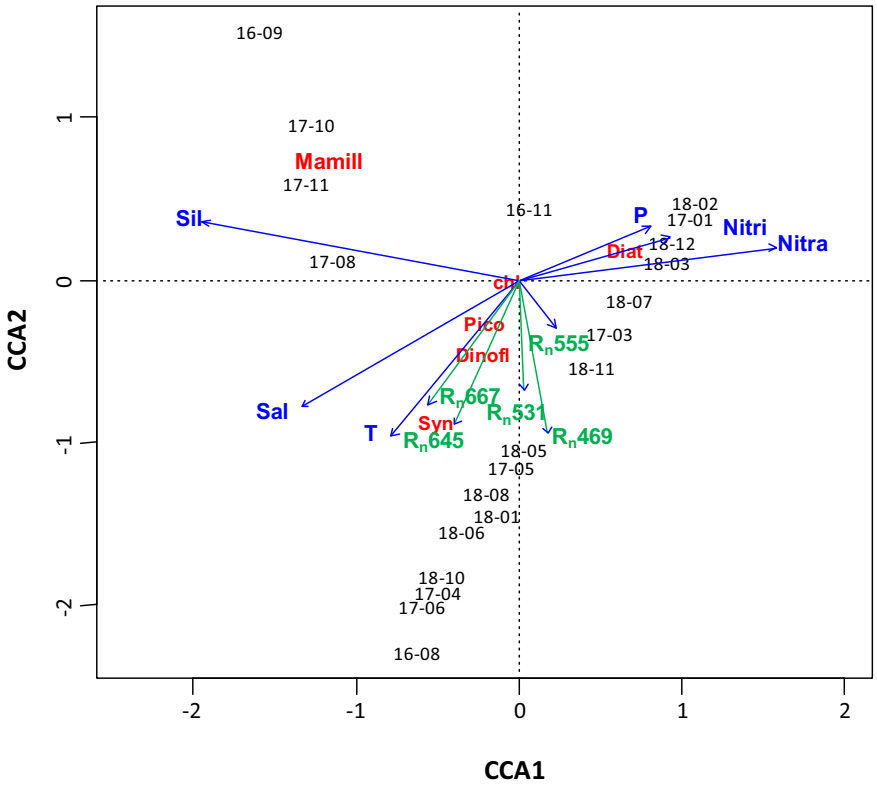

Fig. 7. Biplot of the scores obtained from the Canonical Correspondence Analysis. Environmental variables are shown in blue: T: temperature; Sal: salinity; Sil: silicate; Nitra: nitrate concentration; Nitri: nitrite concentration; P: phosphate. Phytoplankton variables are displayed in red: Chl: chlorophyll *a*; Diat: diatoms; Dinofl: dinoflagellates; Syn: *Synechococcus*; Mamill: Mamiellophyceae; Pico: other picoeukaryotes. Satellite reflectance variables appear in green. The scores of the samples used in the analysis are noted with the sampling date (year-month). (For interpretation of the references to color in this figure legend, the reader is referred to the web version of this article.)

have unique light absorption and backscattering properties determined by their shape, cell structure and pigment composition, which influence their reflectance spectra. Therefore, the observed changes in 2014 could be an indicator of the phytoplankton shifts which, in turn, dealt to the EDAB. Satellite reflectance has been used to remotely identify causative species of blooms (Warmer and Fan, 2013; Simis et al., 2005). Particularly, phytoplankton communities dominated by cyanobacteria have been identified from the unique absorption peaks of phycobilins around 530–550 nm and 620 nm (Roy, 1989) that produce minimum of R_n at 620 nm followed by local maximum at 650 nm (Simis et al., 2005; Wojtasiewicz and Stoń-Egiert, 2016). In fact, the satellite spectral reflectance at these wavebands has been used to measure the

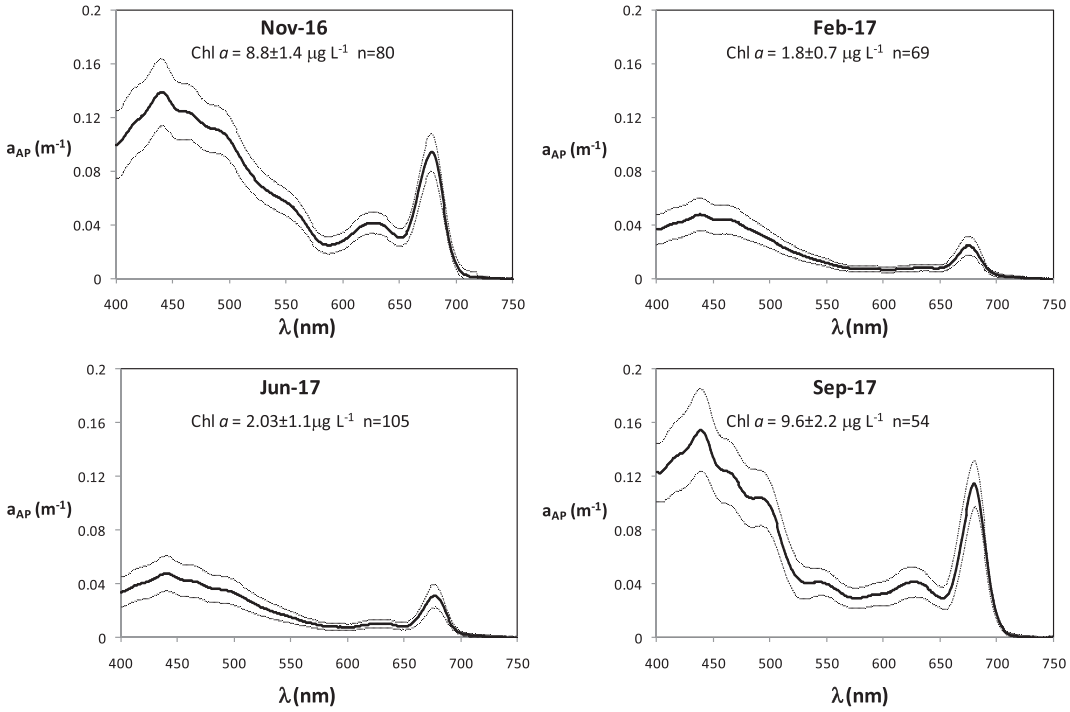

Fig. 8. Phytoplankton absorption spectra averaged (continuous line) ± 1SD (dotted lines). Chlorophyll *a* concentration mean (±SD) and amount of samples analyzed (n) are indicated in each panel.

cyanobacterial bloom magnitude (Mishra et al., 2019). In the Mar Menor, the main change in satellite reflectance consisted of increases in R_n645 that could therefore be attributed to the optical signature of cyanobacteria. Concordantly, the results of the CCA clearly indicate that the abundances of *Synechococcus* in 2016–2018 were tightly related to variability in the blue R_n bands. Furthermore, the absorption spectra obtained from the intensive samplings in 2016–2017 show absorption peaks at 620 nm that can be attributable to cyanobacteria. Note that the non-living matter absorption spectra presented a local minimum at this wavelength which reinforces the hypothesis that any increase in R_n645 might be attributable to phytoplankton. It has to be noted that diatoms could also contribute to increase in reflectance of the blue band due to absorption by chlorophyll c1 and c2; however, the high abundances of diatoms obtained during some monthly sampling periods were not reflected in our R_n values, as demonstrated from the CCA results. Consequently, our data support the hypothesis that the increasing presence of *Synechococcus* featured the start of the EDAB.

The data of abundance and composition of the phytoplankton communities also indicate that the abundance values of *Synechococcus* obtained in our analyses for 2016 (and afterwards) are higher than those ones published previously. Ghai et al. (2012) analyzed the composition of the picoplankton communities in the Mar Menor in 2010 and showed that *Synechococcus* was the only free-living cyanobacterium identified in the lagoon by genetic methods as well as that the phytoplankton community was dominated by dinoflagellates. The abundance of *Synechococcus* reported in that article (estimated by inverted microscopy) is about one order of magnitude lower than the abundance maxima obtained in our analysis (i.e. 5 10^6 cells mL^{-1}). Furthermore, the maximal abundances obtained in our study are comparable with those described for another Mediterranean coastal lagoon located nearby the Mar Menor, the Albufera in Valencia, which has been classified as hypertrophic and whose phytoplankton community is dominated by cyanobacteria (Romo et al., 2008). Our maximal abundances of *Synechococcus* are also close to those observed in other Mediterranean hypertrophic estuaries and coastal lagoons (Caroppo, 2000; Camacho et al., 2003). Based on these results, we conclude that *Synechococcus* had a relevant role in the onset of the EDAB occurred in the Mar Menor as it has been reported for other lagoons affected by this process (Phlips et al., 1999; Glibert et al., 2004).

Irrespectively of the nutrient enrichment suffered by the lagoon during the last decades (which created the necessary environment for stimulating algal growth), the specific factor that triggered the EDAB in the Mar Menor is still unknown. Our data indicate that significant positive anomalies of atmospheric temperature occurred in 2014–2016 when, in contrast, negative anomalies were reduced, indicating that this period was abnormally warm. Our results show that increasing abundance of *Synechococcus* was linked to increase of temperature in 2016–2019. Therefore, this factor would have contributed to the development of the EDABs. Nevertheless, the *Synechococcus* bloom is not necessarily a direct consequence of temperature increasing as this pressure should affect the whole ecosystem. Sunda et al. (2006) and Sunda and Shertzer (2012) have shown that the trophic interactions play a determinant role in the dynamics of the EDABs. According to these authors, competition of phytoplankton species by different nutrient sources (including organic forms) and differential grazing on these species are key factors in development of EDABs. In that sense, Pérez-Ruzafa et al. (2019) pointed out that grazing exerted on phytoplankton by herbivores explains the low levels of Chl *a* in the lagoon before the EDAB, suggesting that loss of predators could have been a key factor in that process. Yet, data supporting this hypothesis have not been presented so far. However, it could be speculated that the predator absence would be a consequence (better than a cause) of the *Synechococcus* bloom. Our data indicate that the initial bloom occurred along with notable changes in the phytoplankton composition possibly modifying the quality and palatability of the herbivore diet.

Previous data of phytoplankton composition in the Mar Menor are scarce but support that the community in 2016–2019 was fairly different compared to previous periods. Gilabert (2001) described abundance up 10^3 cells mL^{-1} of *Cylindrotheca closterium* in summer as well as dominance of *Rhodomonas*, Cryptomonas and *Cyclotella* during the rest of the annual cycle. *Nitzschia* and Cylindrotheca were the most abundant diatoms in our study from August 2016 to April 2017 and occasionally

afterwards; but its abundance peaks were higher by one magnitude order and did not exhibited any seasonal pattern. Furthermore, substantial interannual changes in the patterns of dominance of diatoms and dinoflagellates were produced in 2016–2018. These data indicate that the alteration in the phytoplankton community persisted afterwards the first phase of the EDAB even although abundance of *Synechococcus* decreased. In our study, diatom abundance was related to time periods with higher nitrate concentrations. These results indicate that the mechanisms regulating the phytoplankton community in the Mar Menor, including both nutrient availability and grazing pressure, have been altered substantially in 2016–2019. As an example of this, we reported a substantial reduction of Chl *a* and increasing water clearance in 2018, with values similar to those one observed before the EDAB. This change was interpreted as a recovery of the lagoon ecosystem was occurring (Pérez-Ruzafa et al., 2019). However, Chl *a* increased gradually between March and August 2019 and suddenly in September 2019, when concentrations even higher than those found in 2016 were registered. This latter abrupt increase was linked to a flood occurred in that date. These rapid changes in chlorophyll concentration have not been observed in the lagoon before the EDAB supporting that the homeostatic capacity of the lagoon has been affected substantially.

Supplementary data to this article can be found online at https://doi.org/10.1016/j.marpolbul.2021.111989.

CRediT authorship contribution statement

Mercado JM: Conceptualization, writing, original draft, sample analysis, data collection; **Cortés D**: sample analysis; **Gómez-Jakobsen F**: data acquisition, formal analysis; **García-Gómez C**: sample collection and analysis; **Ouaissa S**: sample analysis; **Yebra L**: conceptualization, review and editing; **Ferrera I.**: conceptualization, review and editing; **Valcárcel-Pérez N**: sample collection; **López M**: sample analysis; **García-Muñoz R**: planning of samplings, sample collection and analysis; **Aranzazu Ramos:** sample collection and analysis; **Bernardeau J**: sample collection and analysis; **Belando MD**: sample collection and analysis; **Fraile-Nuez E**: conceptualization; planning of samplings, review and editing; **Ruiz JM**: conceptualization, management and coordination responsibility for the research activity and execution; sample collection.

Acknowledgements

The samplings and analyses were supported by the projects MEMM (financed by the Spanish Institute of Oceanography), 2-3 ESMAREU (financed by Spanish Ministry of Agriculture, Food and Environment), 10-ESMARES2-C4A2 (financed by Spanish Ministry of Ecological Transition and Demographic Challenge) and UMBRAL (CTM2017-86695-C3-2-R; financed by the National Plan of Research of the Spanish Government). M.D.B., J.B.E. and N.V.P. were supported by a contract within the Program *Personal Técnico de Apoyo* funded by the Ministry of Economy and Competitiveness. We acknowledge logistical support provided by President and Staff of the harbours Club Nautico Lo Pagán, Club Náutico La Puntica and Centro de Actividades Náuticas (San Pedro del Pinatar, Murcia, Spain). We thank Regional Government of Murcia, and national authorities (MITECO) for permissions. We thank Project EUROGEL (Grant Agreement ID: EVK3-CT-2002-00074) and Spanish Meteorological Agency (AEMET) for providing data.

References

Belando, M.D., Bernardeau-Esteller, J., Paradinas, I., Ramos-Segura, A., Garcia-Muñoz, R., Garcia-Moreno, P., Marin-Guirao, L., Ruiz, J.M., 2019a. Assessment of long-term interaction between an opportunistic macroalga and a native seagrass in a Mediterranean coastal lagoon. Front. Mar. Sci. Conference Abstract: XX Iberian Symposium on Marine Biology Studies (SIEBM XX). https://doi.org/10.3389/conf.fmars.2019.08.00190.

Belando, M.D., Ruiz, J.M., Muñoz, R.G., Segura, A.R., Esteller, J.B., Casero, J.J., Guirao, L.M., Moreno, P.G., Navarro, I.F., Nuez, E.F., Mercado, J.M., 2019b. Collapse of macrophytic communities in a eutrophicated coastal lagoon. Front. Mar. Sci. Conference Abstract: XX Iberian Symposium on Marine Biology Studies (SIEBM XX). https://doi.org/10.3389/conf.fmars.2019.08.00192.

Camacho, A., Picazo, A., Miracle, M.A., Vicente, E., 2003. Spatial distribution and temporal dynamics of picocyanobacteria in a meromictic karstic lake. Arch. Hydrobiol. 148, 171–184.

Caroppo, C., 2000. The contribution of picophytoplankton to community structure in a Mediterranean brackish environment. J. Plankton Res. 22, 381–397.

Carreño, M.F., 2015. Seguimiento de los Cambios de usos y su influencia en las comunidades y hábitats naturales en la cuenca del Mar Menor, 1988–2009, con el uso de SIG y teledetección. Universidad de Murcia, Tesis Doctoral.

Cleveland, J.S., Weidemann, A.D., 1993. Quantifying absorption by aquatic particles: a multiple scattering correction for glass-fiber filters. Limnol. Oceanogr. 38, 1321–1327.

Cloern, J.E., 2001. Our evolving conceptual model of the coastal eutrophication problem. Mar. Ecol. Prog. Ser. 210, 223–253.

Erena, M., Domínguez, J.A., Aguado-Jiménez, F., Soria, J., García-Galiano, S., 2019. Monitoring coastal lagoon water quality through remote sensing: the Mar Menor as a case study. Water 11, 11–1468.

Fertig, B., O'Neil, J.M., Beckert, K.A., Cain, C.J., Needham, D.M., Carruthers, T.J.B., Dennison, W.C., 2013. Elucidating terrestrial nutrient sources to a coastal lagoon, Chincoteague Bay. Maryland USA. Estuar. Coast. Shelf Sci. 116, 1–10.

Fraile-Nuez, E., Machíz, F., Santana-Casiano, J.M., González-Dávila, M., Antón, J., Domíguez-Llánez, J.F., Mercado, J.M., Cortés, D., Yebra, L., Gómez-Jakobsen, F., García-Gómez, C., Valcárcel, N., Gómez-Ballesteros, M., Gómez, F., González-Barberá, G., Santos-Echeandía, J., García-Muñoz, R., Ramos-Segura, A., Bernardeu-Esteller, J., Belando-Torrentes, M.D., Garrido-Faustino, S., Conde-Caño, R.M., Ruíz-Fernández, J.M., 2018. Informe de evaluación y estado actual del Mar Menor en relación al proceso de eutrofización y sus causas. Informe de asesoramiento técnico del Instituto Español de Oceanografía (IEO). 145 pp.

Fuentes, V., Straehler-Pohl, I., Atienza, D., Franco, I., Tilves, U., Gentile, M., Acevedo, M., Olariaga, A., Gili, J.M., 2011. Life cycle of the jellyfish *Rhizostoma pulmo* (Scyphozoa: Rhizostomeae) and its distribution, seasonality and inter-annual variability along the Catalan coast and the Mar Menor (Spain, NW Mediterranean). Mar. Biol. 158, 2247–2266.

García-Oliva, M., Marcos, C., Umgiesser, G., McKiver, W., Ghezzo, M., De Pascalis, F., Pérez-Ruzafa, A., 2019. Modelling the impact of dredging inlets on the salinity and temperature regimes in coastal lagoons. Ocean Coast. Manag. 180, 104913.

Ghai, R., Hernández, C.M., Picazo, A., Mizuno, C.M., Ininbergs, K., Díez, B., Valas, R., DuPont, C.L., McMahon, K.D., Camacho, A., Rodriguez-Valera, F., 2012. Metagenomes of Mediterranean coastal lagoons. Sci. Reports PMID 22778901.

Gilabert, J., 2001. Seasonal plankton dynamics in a Mediterranean hypersaline coastal lagoon: the Mar Menor. J. Plankton Res. 23, 207–218.

Glibert, P.M., Heil, C.A., Hollander, D., Revilla, M., Hoare, A., Alexander, J., Murasko, S., 2004. Evidence for dissolved organic nitrogen and phosphorus uptake during a cyanobacterial bloom in Florida Bay. Mar. Ecol. Prog. Ser. 280, 73–83.

Glibert, P.M., Boyer, J., Heil, C., Madden, C., Sturgis, B., Wazniak, C., 2010. Blooms in lagoons: different from those of river-dominated estuaries. In: Kennish, M., Paerl, H. (Eds.), Coastal Lagoons: Critical Habitats of Environmental Change. Taylor and Francis, Boca Raton, pp. 91–114.

Guiry, M.D. & Guiry, G.M. 2020. *AlgaeBase*. World-wide electronic publication, National University of Ireland, Galway. https://www.algaebase.org; searched on 15 December 2020.

Liu, H., Buskey, E.J., 2000. Hypersalinity enhances the production of extracellular polymeric substance (eps) in the Texas brown tide alga, *Aureoumbra lagunensis* (Pelagopnyceae). J. Phycol. 36, 71–77.

Lloret, J., Marín, A., Marín-Guirao, L., 2008. Is coastal lagoon eutrophication likely to be aggravated by global climate change? Est. Coast. Shelf Sci. 78, 403–412.

Lomas, M.W., Kana, T.M., MacIntyre, H.L., Cornwell, J.C., Nuzzi, R., Waters, R., 2004. Interannual variability of *Aureococcus anophagefferens* in Quantuck Bay. Long Island: natural test of the DON hypothesis. Harmful Algae. 3, 389–402.

López-Ballesteros, A., Senent-Aparicio, J., Srinivasan, R., Pérez-Sánchez, J., 2019. Assessing the impact of best management practices in a highly anthropogenic and ungauged watershed using the SW model: a case study in the El Beal Watershed (Southeast Spain). Agronomy 9, 576.

Majaneva, M., Rintala, J.M., Hajdu, S., Hällfors, S., Hällfors, G., Skjevik, A.T., Gromisz, S., Kownacka, J., Busch, S., Blomster, J., 2012. The extensive bloom of alternate-stage *Prymnesium polylepis* (Haptophyta) in the Baltic Sea during autumn–spring 2007–2008. Eur. J. Phycol. 47, 310–320.

Más-Hernández, J.M., 1996. El Mar Menor. Relaciones, diferencias y afinidades entre la laguna costera y el mar mediterraneo adyacente. Ph.D. Thesis. Universidad Autónoma de Madrid, España.

McGlathery, K.J., Sundbäck, K., Anderson, I.C., 2007. Eutrophication in shallow coastal bays and lagoons: the role of plants in the coastal filter. Mar. Ecol. Prog. Ser. 348, 1–18.

Mercado, J.M., Ramírez, T., Cortés, D., 2008. Changes in nutrient concentration induced by hydrological variability and its effect on light absorption by phytoplankton in the Alborán Sea (Western Mediterranean Sea). J. Mar. Syst. 71, 31–45.

Michaloudi, E., Moustaka-Gouni, M., Gkelis, S., Pantelidakis, K., 2008. Plankton community structure during an ecosystem disruptive algal bloom of *Prymnesium parvum*. J. Plankton Res. 31, 301–309.

Mishra, S., Stumpf, R.P., Schaefer, B.A., Werdell, P.J., Loftin, K.A., Meredith, A., 2019. Merasurement of cyanobacterial bloom magnitude using satellite remote sensing. Sci. Rep. 9, 18310. https://doi.org/10.1038/s41598-019-54453-y.

Oksanen, J., Blanchet, F.G., Kindt, R., Legendre, P., Minchin, P.R., O'Hara, R.B., Simpson, G.L., Solymos, P., Stevens, M.H.H. and Wagner, H., 2014. Vegan: community ecology package. R Package Version 2.2-0.

Pérez-Ruzafa, A., Marcos, C., Gilabert, J., 2005. The ecology of the Mar Menor coastal lagoon: a fast changing ecosystem under human pressure. In: Gönenç, I.E., Wolflin, J. P. (Eds.), Coastal Lagoons: Ecosystem Processes and Modeling for Sustainable Use and Development, CRC Press. Boca Ratón, Florida, pp. 392–422.

Pérez-Ruzafa, A., Campillo, S., Fernández-Palacios, J.M., García-Lacunza, A., García-Oliva, M., Ibañez, H., Navarro-Martínez, P.C., Pérez-Marcos, M., Pérez-Ruzafa, I.M., Quispe-Becerra, J.I., Sala-Mirete, A., Sánchez, O., Marcos, C., 2019. Long-term dynamic in nutrients, chlorophyll *a*, and water quality parameters in a coastal lagoon during a process of eutrophication for decades, a sudden break and a relatively rapid recovery. Front. Mar. Sci. 11 https://doi.org/10.3389/fmars.2019.00026.

Phlips, E.J., Badylack, S., Lynch, T.C., 1999. Blooms of the picoplanktonic cyanobacterium Synechococcus in Florida Bay, a subreopical inner-shelf lagoon. Limnol. Oceanogr. 44, 1166–1175.

R Core Team, 2013. R: a language and environment for statistical computing. In: R Foundation for Statistical Computing. Austria. URL, Vienna. http://www.R-project.org/.

Ramírez, T., Cortés, D., Mercado, J.M., Vargas-Yáñez, M., Sebastián, M., Liger, E., 2005. Seasonal dynamics of inorganic nutrients and phytoplankton biomass in the NW Alboran Sea. Estuar. Coast. Shelf Sci. 65, 654–670.

Romo, S., García-Murcia, A., Villena, M.J., Sánchez, V., Ballester, A., 2008. Albufera de Valencia and implications for its ecology, management and recovery. Limnetica 27, 11–28.

Roy, S., 1989. HPLC-measured chlorophyll-type pigments during a phytoplankton spring bloom in Bedford Basin (Canada). Mar. Ecol. Prog. Ser. 55, 279–290.

Ruiz, J.M., Albentosa, M., Belando, M.D., Aboal, M., et al., 2016. Programa de seguimiento de la eutrofización en la laguna costera del Mar Menor. Report of the Project MEMM.. Spanish Institute of Oceanography, Madrid, Spain, 33 pp.

Simis, S.G., Peters, S.W., Gons, H.J., 2005. Remote sensing of the cyanobacterial pigment phycocyanin in turbid inland water. Limnol. Oceanogr. 50, 237–245.

Soria, J., Caniego, G., Hernández-Sáez, N., Erena, M., 2019. Phytoplankton distribution in Mar Menor Coastal Lagoon (SE Spain) during 2017. Preprints 2019120277.

Sunda, W.G., Shertzer, K.W., 2012. Modeling ecosystem disruptive algal blooms: positive feedback mechanisms. Mar. Ecol. Prog. Ser. 447, 31–47.

Sunda, W.G., Graneli, E., Gobler, C.J., 2006. Positive feedback and the development and persistence of disruptive algal blooms. J. Phycol. 42, 963–974.

Terrados, J., Ros, J., 1991. Production dynamics in a macrophyte-dominated ecosystem the Mar Menor coastal lagoon (SE Spair). Oecologia Aquat. 10, 255–270.

Tomas, C.R., 1997. Identifying Marine Phytoplankton. Academic Press Limited, London (858 pp.).

Trice, T.M., Glibert, P.M., Lea, C., Van Heukelem, L., 2004. HPLC pigment records provide evidence of past blooms of *Aureococcus anophagefferens* in the Coastal Bays of Maryland and Virginia. USA. Harmful Algae. 3, 295–304.

Utermöhl, H., 1958. Zur Vervollkommnung der quantitativen Phytoplankton-Methodik. Mitt. int Verein. Limnol. 9, 1–38.

Vaulot, D., Courties, C., Partensky, F., 1989. A simple method to preserve oceanic phytoplankton for flow cytometric analyses. Cytometry 10, 629–635.

Warmer, R.A., Fan, C., 2013. Optical spectra of phytoplankton cultures for remote sensing applications: focus on harmful algal blooms. Int. J. Environ. Devel. 4, 94–98.

Wojtasiewicz, B., Stoń-Egiert, J., 2016. Bio-optical characterization of selected cyanobacteria strains present in marine and freshwater ecosystems. J. Appl. Phycol. 28, 2299–2314.

Zhang, X., Kan, J., Wang, J., Gu, H., Ju, J., Zhao, Y., Sun, J., 2015. Fist Record of a Large-Scale Bloom Causing Causes Species *Nannochloropsis granulata* ole1430–1441.